Stabilization of Orthorhombic Phase in Single-Crystal ZnSnN₂ Films

Nancy Senabulya¹, Nathaniel Feldberg^{2,a)}, Robert. A. Makin³, Yongsoo Yang^{4,b),} Guangsha Shi⁵, Christina M. Jones¹, Emmanouil Kioupakis⁵, James Mathis¹, Roy Clarke^{1,4} and Steven M. Durbin³

We report on the crystal structure of epitaxial ZnSnN₂ films synthesized via plasma-assisted vapor deposition on (111) yttria stabilized zirconia (YSZ) and (001) lithium gallate (LiGaO₂) substrates. X-ray diffraction measurements performed on ZnSnN₂ films deposited on LiGaO₂ substrates show evidence of single-crystal, phase-pure orthorhombic structure in the Pn2₁a symmetry [space group (33)], with lattice parameters in good agreement with theoretically predicted values. This Pn2₁a symmetry is imposed on the ZnSnN₂ films by the LiGaO₂ substrate, which also has orthorhombic symmetry. A structural change from the wurtzite phase to the orthorhombic phase in films grown at high substrate temperatures ~550°C and low values of nitrogen flux~10⁻⁵ Torr is observed in ZnSnN₂ films deposited on YSZ characterized by lattice contraction in the basal plane and a 5.7% expansion of the out-of-plane lattice parameter.

Heterovalent ternary compounds (HTCs) offer a unique opportunity to tune their electrical properties through structural changes of the crystal lattice. Specifically, in some HTCs, the band gap of the material can be controlled by introducing disorder into the cation sublattice. Disorder-induced band-gap tuning was experimentally first reported in GaInP₂ films where introduction of Sb during growth led to the random placement of cations in the Ga-In sublattice, leading to an increase of up to 0.135 eV in the direct band gap [1]. Recently, theoretical calculations of the ZnSnP₂ band structure predicted a 0.95 eV reduction of the band gap with a fully disordered Zn-Sn sublattice [2]. Experimentally, however, disordering of the cation sublattice has so far only achieved a 0.3 eV reduction in the band gap with the

^b Now at Department of Physics and Astronomy, University of California, Los Angeles, CA 90095-1547, USA

¹Applied Physics Program, University of Michigan, Ann Arbor, Michigan 48109, USA

²Department of Physics, University at Buffalo, Buffalo, New York 14260, USA

³Department of Electrical and Computer Engineering, Western Michigan University, Kalamazoo, Michigan, 49008-5329, USA

⁴Department of Physics, University of Michigan, Ann Arbor, Michigan 48109, USA

⁵Department of Materials Science and Engineering, University of Michigan, Ann Arbor, Michigan 48109, USA

^a Present address: Institut Jean Lamour (University of Lorraine), France

apparent differences in band-gap narrowing attributed to variations in cation-sublattice disorder [2,3].

Another candidate material for band-gap tuning through controlled disorder of the cation sublattice is the related material ZnSnN₂, an earth-abundant semiconductor. The band gap of ZnSnN₂ has been reported in multiple theoretical studies ranging from 1.4 to 2 eV [4,5,6]. Density functional theory (DFT) calculations predict that varying degrees of disorder on the Zn-Sn sublattice will shrink the band gap from 2.0 eV to 1.0 eV [7,8], a range that makes ZnSnN₂ a prime candidate for photovoltaic applications [9,10,11] and light-emitting diode technology [12].

Ordering in the cation sublattice in ZnSnN₂, in addition to increasing the band gap, changes the symmetry of the crystal structure. According to DFT predictions [8], fullycation-ordered ZnSnN2 is orthorhombic, while a fully disordered cation sublattice leads to a wurtzite ZnSnN₂ structure. Recently, however, another model of disorder has been proposed for this system that asserts the band-gap is relatively insensitive to disorder and the lattice structure remains orthorhombic even in disordered states [13]. In this study, Quayle et al. propose a hypothesis for disorder in ZnSnN₂ based on the stacking of two orthorhombic phases, Pna2₁ and Pmc2₁, normal to the basal plane. The motivation for this alternate hypothesis of disorder came from conflicting results obtained from vapor-liquid-solid-grown samples [14]. Using photoluminescence, the measured band gap of these samples was 1.7 eV, consistent with the DFT predicted band gap for the orthorhombic phase of ZnSnN₂. X-ray diffraction (XRD) measurements on the same samples, however, were consistent with a disordered wurtzite lattice structure, which has a predicted band gap of 1.0 eV [8]. These variations in the cation-sublattice ordering of ZnSnN2 and the lack of consensus about the structure and optoelectronic properties of this material call for more detailed experimental studies.

We have grown a series of ZnSnN₂ films via plasma-assisted molecular beam epitaxy. Through a systematic variation of growth parameters and choice of different substrates, we were able to obtain both the predicted wurtzite and orthorhombic lattice structures for ZnSnN₂. X-ray measurements suggest that the cation arrangement in the measured wurtzite films is consistent with the disorder due to random placement of Zn and Sn atoms on the cation sublattice [8]. Although a theoretical study [13] predicts that this type of random disorder would not be favored due to octet-rule violations that result in a high energy of formation, recent experimental work by Fioretti et al. reported on the wurtzitic structure of

ZnSnN₂ films with band-gap values close to 1.0 eV; these samples were grown using a combinatorial RF co-sputtering approach [15]. It would seem, therefore, that the nature of cation disorder in ZnSnN₂, whether originating from layer-stacking polytypes [13] or random decoration of the cation sublattice, is worthy of further research.

Single-crystal thin films of ZnSnN₂ were grown on (111) YSZ and (001) LiGaO₂ substrates, which were cleaned prior to growth via a standard three-step solvent cleaning sequence consisting of trichloroethane, acetone, and methanol. The films were grown in a Perkin Elmer 430 molecular beam epitaxy (MBE) system using conventional effusion cells for Zn and Sn evaporation; the Zn and Sn fluxes were measured using a quartz crystal microbalance. Active nitrogen was created using an Oxford Applied Research HD25 inductively-coupled RF plasma source equipped with a 256-hole aperture plate, with electrostatic ion removal. The film growth was monitored *in situ* using a 20 kV Staib Instruments reflection high-energy electron diffraction (RHEED) system along with a KSA 400 image acquisition and analysis package.

We performed extensive x-ray diffraction (XRD) measurements on the epitaxial films using synchrotron radiation at the Advanced Photon Source. Unit-cell refinement measurements for the ZnSnN₂ films were performed by fitting at least twenty (20) film reflections using film Bragg-peak positions obtained from Kappa diffractometer angle calculations. For ZnSnN₂ films grown on (001) LiGaO₂, measurements revealed lattice-constant values of a = 5.9557(3) Å, b = 5.5778(3) Å and c = 6.8852(3) Å with extinctions corresponding to the Pn2₁a symmetry [space group (33)]. We note that the unit cell lattice parameters of orthorhombic films, P56 and P57 are, on average, within 2% and 1%, respectively, of the results on polycrystalline ZnSnN₂ films [14]. It is also clear from Table 1 that the unit-cell volume of P56 shows a difference of less than 3% with respect to the DFT results, while P57 has a less than 1% difference with DFT. We attribute the variation in unit cell parameters between these two orthorhombic films to the differences in growth conditions. The films were deposited at Sn effusion-cell temperatures of 1040°C and 1050°C for P56 and P57, respectively.

The unit-cell lattice parameters obtained from XRD measurements and DFT calculations are compared in Table 1. Our first-principles calculation studies based on DFT were used to

determine the optimized structure of the 16-atom orthorhombic ZnSnN2 unit cell, with projector-augmented waves [16] and a cutoff of 350 eV as implemented in the Vienna Ab initio Simulation Package (VASP) [17]. The calculations use the Perdew-Burke-Exchange (PBE) [18] functional for the exchange-correlation potential. DFT-computed lattice parameters were found to be a = 5.914 Å, b = 6.812 Å and c = 5.542 Å, referenced to the Pna2₁ symmetry group [space group (33)]. Comparing the experimentally determined lattice constants for single-crystal ZnSnN₂ films grown on LGO, referenced to the Pna2₁ symmetry with results from DFT calculations (Table 1) we note that there are 1.1%, 0.7% and 0.65% differences between the experimental and the calculated lattice constants a, b and c, respectively. These differences can be attributed to the significant compressive epitaxial strain in the ZnSnN₂ films induced by the substrate (the DFT model assumes a fully relaxed bulk ZnSnN₂ structure), as well as the typical 1% accuracy of DFT in predicting lattice constants. The film lattice constants obtained are also in good agreement with LDA calculations [19] showing differences with our experimental results of 1.9% and 1.8% in a and b lattice constants, respectively, while the out-of-plane lattice constant, c, of P56 is in good agreement (~0.04% difference).

TABLE I: Experimentally determined lattice parameters for our orthorhombic single-crystal ZnSnN₂ (ZSN) films referenced in the Pna2₁ symmetry compared with experimentally determined lattice constants for polycrystalline ZnSnN₂ films and results from different computational methods. Ideal axial ratios are $b/a_w = 1.732$ and $c/a_w = \sqrt{(8/3)} = 1.633$, $a_w = a/2$.

	Orthorhombic (Calculated)				
	P56 ^a (ZSN/LGO)	P57 ^b (ZSN/LGO)	*Polycrystalline- ZSN	PBE, this work	**LDA
a (Å)	6.8852(3)	6.8115(3)	6.753	6.812	6.76
b (Å)	5.9557(3)	5.9544(3)	5.842	5.914	5.85
c (Å)	5.5778(3)	5.4583(3)	5.462	5.542	5.58
a _w (Å)	3.4426	3.4059	3.3765	3.406	3.38
b/a _w	1.730	1.748	1.73	1.736	1.731
c/a _w	1.620	1.603	1.618	1.627	1.651
Volume (Å)	228.724	221.380	215.48	223.3	220.667

^{a, b} Lattice constants given are referenced to the Pna2₁ structure.

Punya et al. [19] suggested that the orthorhombic unit cell of II-IV- N_2 compounds can be viewed as a $2\times\sqrt{3}$ superstructure of the wurtzite structure along orthohexagonal axes. The orthorhombic unit cell in this instance is defined by choosing $a_{ortho}=2a_w$ and $b_{ortho}\approx\sqrt{3}a_w$ with axial ratio b/a_w referenced to the orthorhombic structure equal to 1.732 and $c/a_w=1.633$.

^{*}from Ref [14]

^{**}from Ref [19]

The wurtzite structure is assumed to have an underlying hexagonal Bravais lattice from which the orthorhombic superstructure is derived. The comparison to the ideal axial ratios in the hexagonal close packed (hcp) structure is made to illustrate the analogy between the cation-sublattice ordering in the orthorhombic structure and the ABAB stacking in the hcp structure. Our measurements show a less than 1% difference between the ideal axial ratios and experimental values in the orthorhombic films. The b/a_w ratio is slightly overestimated in the experimental results for P57 and the calculated DFT results, while the c/a_w ratio is underestimated in the experimental results by less than 2%.

Synchrotron x-ray diffraction experiments were carried out at beam lines 13-BM-C, 33-ID-D, and 33-BM-C of the Advanced Photon Source. A monochromatic X-ray beam at 15 keV was used to probe the film's crystal structure and its epitaxial relationship with the substrate. The beam spot size was optimized at 270µm x 30µm in the horizontal and vertical directions respectively. To resolve the symmetry of the ZnSnN₂ films, high-resolution three-dimensional reciprocal space maps (3D RSMs) were measured around high-order film Bragg peaks. Using a PILATUS 100K area detector [20,21], the intensity distribution around each peak was measured in a series of single scans along the L-direction as a set of two-dimensional reciprocal space slices. These were then used to reconstruct the 3D RSMs [22].

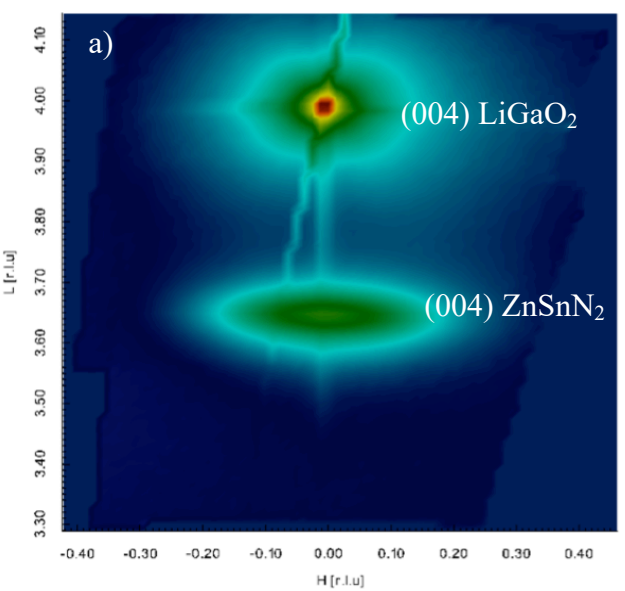


FIG 1: (a) (004) RSM of ZnSnN₂. H and L are given in reciprocal lattice units of the LGO substrate.

In order to understand the epitaxial relationship between the ZnSnN₂ films and LiGaO₂ substrates, and hence the role of strain on the structure of the films, 3D reciprocal space maps (RSMS) were reconstructed around high-order-specular and off-specular film Bragg peaks. Fig 1(a) shows a high-resolution, XRD reciprocal space map around the (004) reflection of

the orthorhombic phase. The (004) RSM shows clear evidence of single domain $ZnSnN_2$ epitaxy, indicated by the absence of any splitting in both film and substrate reflections. The reciprocal space maps of the (102) and ($\overline{1}02$) film Bragg peaks in Figure 2(a) and 2(b)

respectively show partial substrate-induced strain in the film with the bulk of the film relaxed. The center of the film Bragg peak occurs at $H = \pm 0.93$ in substrate reciprocal lattice units, indicating ~97% in-plane relaxation. This relaxation is consistent with film lattice constants approaching the bulk values that have been predicted through our DFT calculations and published theoretical lattice constants, as shown in Table I. The maximum compressive strain along the [100] direction needed for the film to be in registry with the substrate (lattice mismatch) is ~7.4% based on calculations from fitted ZnSnN₂ and LiGaO₂ lattice parameters. We attribute the film relaxation to having relatively thick films (~125nm), which may reduce the substrate-induced strain effect on the film. We also note here that the (102) and ($\overline{1}$ 02)

ZnSnN₂ symmetry-equivalent Bragg peaks in Figure 2(a) and 2(b) appear at slightly different positions along the L direction due to the significant substrate miscut \sim 1.2°. Pole figure measurements were carried out to verify the two-fold symmetry of the orthorhombic films and the results can be found in the supplementary section of this manuscript.

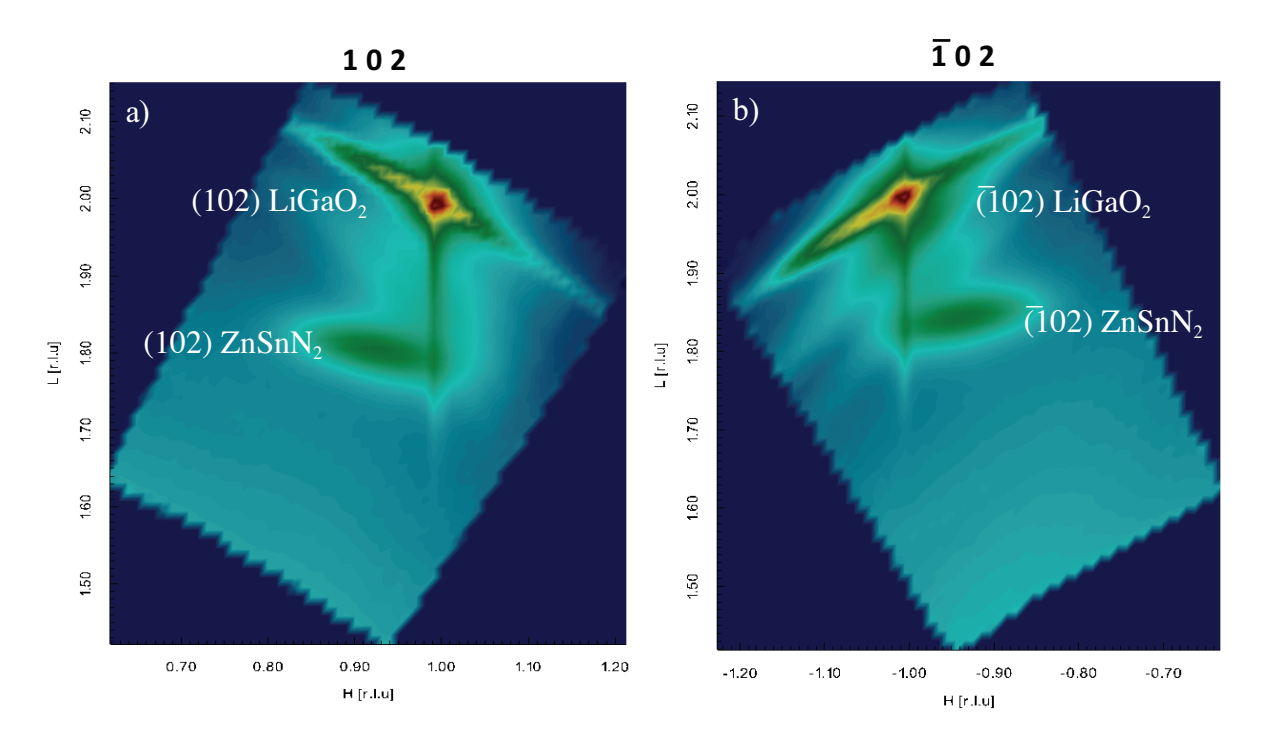


FIG 2: RSMs through the $ZnSnN_2(102)$ and $(\overline{\mathbf{1}}02)$ symmetry-equivalent Bragg peaks. H and L are given in reciprocal lattice units of LGO substrate.

The disordered phase of ZnSnN₂, associated with a random distribution of Zn and Sn atoms on the cation sublattice, has been studied in multiple reports. Feldberg et al. [24] reported a unit cell of a = 3.383 Å, b = 3.379 Å and c = 5.567 Å in monoclinic films (they ascribed small angular distortions to monoclinic symmetry). X-ray diffraction measurements on ZnSnN₂ films grown on (111) YSZ between 250°C - 450°C (e.g., P64 in Table II) revealed a wurtzite unit cell with lattice constants a = 3.3882(3) Å b = 3.3832(3) Å c = 5.5274(3) Å in good agreement with experimental results reported in Feldberg et al. [23].

Table II: Experimentally fitted lattice constants for $ZnSnN_2$ films deposited on (111) YSZ substrate referenced in the wurtzite structure.

TO WILLIAM DEL WOOD OF								
	a(Å)	b(Å)	c(Å)	c/a _w	$V(Å^3)$			
P64	3.3882(3)	3.3832(3)	5.5274(3)	1.631	54.872			
P71	3.366(2)	3.366(2)	5.842(3)	1.736	57.322			

By systematically varying the growth conditions, a structural phase transition from the wurtzite to orthorhombic structure was observed as shown in Table II. Film P64 was deposited under a substrate temperature of 450 °C and a nitrogen pressure of 10⁻⁵ Torr while film P71 was deposited under a substrate temperature of 550 °C and a nitrogen pressure of 10^{-5} Torr. We note that there is a contraction in the basal plane of $\sim 0.65\%$ and a relatively large expansion in the out-of-plane direction of ~5.7% for the P71 film grown at higher substrate temperatures and a lower value of nitrogen pressure. This phase transition as shown in Figure 3(b) is associated with peak splitting along the [10L], [01L] and [11L] directions. The splitting is a direct result of the breaking of symmetry in the basal plane of the wurtzite unit cell and the occurrence of unequal in-plane axes characteristic of the orthorhombic structure with $a \neq b \neq c$. The six-fold diffraction pattern in Figure 3(a) shows the (102), (112) and (012) peaks of wurtzite ZnSnN₂; these three respective Bragg peaks are shown doubly split in Figure 3(b) with a corresponding twelve peak diffraction pattern observed. We also note that the in-plane lattice constant $a \sim 6.732$ Å for film P71 when referred to the orthorhombic lattice, is in good agreement with the in-plane lattice constant given in ref [14] for the orthorhombic Pna2₁ symmetry and within 2% of the fitted lattice parameters for the ZnSnN₂ films grown on LiGaO₂ discussed in this work. Interestingly, the value of the c/a_w ratio of the orthorhombic P71 film when referenced in the hexagonal lattice frame is ~1.736, a value 6.3% larger than the "ideal" wurtzite axial ratio of 1.633 and in good agreement with the b/a_w ratio given in our DFT calculations for the orthorhombic Pna2₁ symmetry.

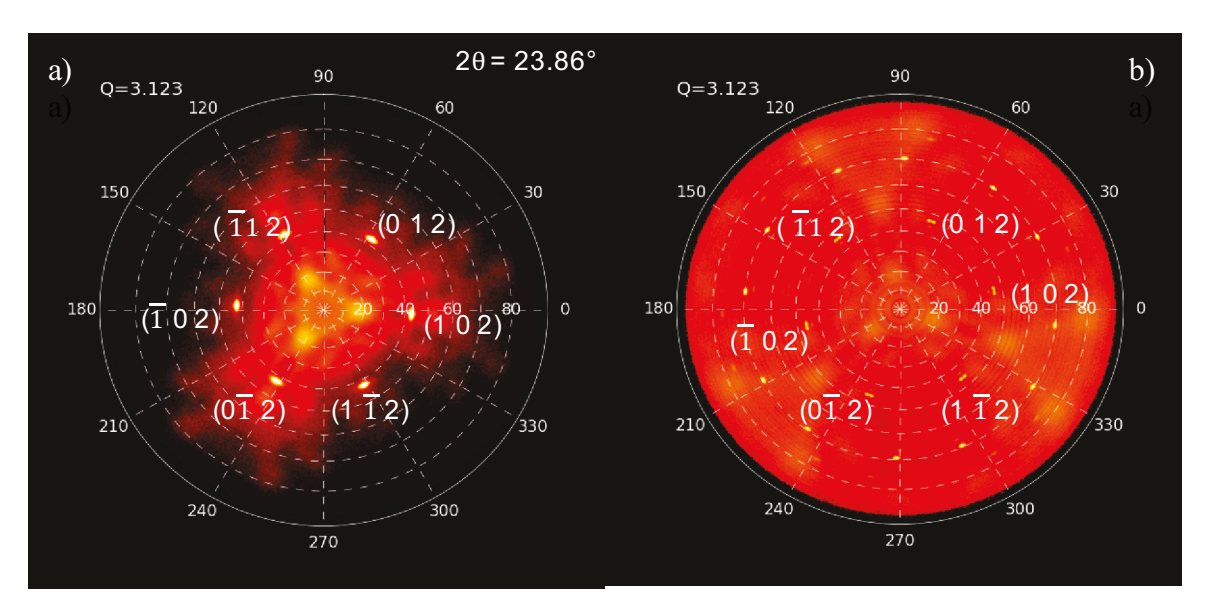


FIG 3: (102), (112) and (012) pole figure of $ZnSnN_2$ films grown on (111) YSZ substrate. (a) Wurtzite film (P64) grown at a substrate temperature of 450 °C. (b) Orthorhombic $ZnSnN_2$ film (P71) grown at a substrate temperature of 550 °C.

This sample (P71), which is evidently of higher crystal quality than that grown on LGO (c.f., Figures 3(b) and supplementary figure 3(a) shows a clear distortion from the wurtzite phase and suggests that the large expansion in the c-axis spacing may be associated with the ordering of the heterovalent cations in the orthorhombic phase. These findings are consistent with studies on the related material ZnSnP₂ showing that higher growth temperatures are more likely to produce a more ordered film than lower growth temperatures [24]. This has been explained as a consequence of the dominance of kinetic processes in low-temperature MBE [24].

In summary, our experimental work has shown definitive x-ray evidence of the first reported case of single-crystal, single-domain orthorhombic films of ZnSnN₂ grown epitaxially on (001) LiGaO₂ substrates with the Pn2₁a symmetry, demonstrating that the orthorhombic phase of ZnSnN₂ is stabilized by growing ZnSnN₂ films on an orthorhombic substrate such as LiGaO₂. By tuning growth conditions, a structural phase transition from the wurtzite to orthorhombic phase can be achieved in films grown on (111) yttria-stabilized zirconia. The findings of this study open a door for research into the optoelectronic properties of the ordered phase of ZnSnN₂ and will be especially useful in future applications of ZnSnN₂ films in photovoltaics and solid-state lighting. Work is ongoing to determine the role of growth conditions and film thickness, including epitaxial strain effects, on the crystal structure of ZnSnN₂ thin films.

ACKNOWLEDGEMENTS

This work is supported in part by the National Science Foundation Grant No. DMR-1410915 (Program Manager Charles Ying) and at UM by NSF Grant No. DMR 10006835. The DFT calculations were supported by the National Science Foundation CAREER award through Grant No. DMR-1254314. N. Senabulya acknowledges funding from the Schlumberger Faculty for the Future Grant and thanks V. Stoica and H. Ferguson for thoughtful discussions and help with experiments at APS. C. Jones acknowledges support by the National Science Foundation Graduate Research Fellowship Program through Grant No. DGE-1256260. The authors also wish to thank Brian Durant for his assistance with film growth. X-ray diffraction experiments were performed at sectors 13-BMC (GeoSoilEnviroCARS), 33-IDD (XSD), and 33-BMC (XSD) at the APS. Excellentbeam line support by Christian M. Schlepütz, P. Eng., J. Stubbs, Z. Zhang, E. Karapetrova, and the staff of the APS is gratefully acknowledged. GeoSoilEnviroCARS is supported by the National Science Foundation - Earth Sciences (EAR-0622171) and Department of Energy – Geosciences (DE-FG02-94ER14466). The use of the APS was supported by the U.S. Department of Energy, Office of Science, Office of Basic Energy Sciences, under Contract No. DE-AC02-06CH11357. This research used resources of the National Energy Research Scientific Computing Center, a DOE Office of Science User Facility supported by the Office of Science of the U.S. Department of Energy under Contract No. DE-AC02-05CH11231.

REFERENCES

- [1] Shurtleff, J. K., Lee, R. T., Fetzer, C. M., Stringfellow, G. B. (1999). Applied Physics Letters, 75, 1914-1916.
- [2] Scanlon, D. O., Walsh, A. (2012). Applied Physics Letters, 100, 251911.
- [3] St-Jean, P., Seryogin, G. A., & Francoeur, S. (2010). Applied Physics Letters, 96, 231913
- [4] N. Feldberg, B. Keen, J. D. Aldous, D. Scanlon, P. A. Stampe, R. Kennedy, R. Reeves, T. D. Veal, and S. Durbin, ZnSnN2: A new earth-abundant element semiconductor for solar cells, in Proceedings of the 38th Photovoltaic Specialists Conference (PVSC) (IEEE, New York, NY, 2012), pp. 2524–2527
- [5] L. Lahourcade, N. C. Coronel, K. T. Delaney, S. K. Shukla, N. A. Spaldin, and H. A. Atwater, Structural and optoelectronic characterization of RF sputtered ZnSnN₂, Adv. Mater. 25, 2562 (2013).
- [6] Punya, W. R. L. Lambrecht, and M. van Schilfgaarde, Quasiparticle band structure of Zn IV-N₂ compounds, Phys. Rev. B 84, 165204 (2011).
- [7] N. Feldberg, J. D. Aldous, W. M. Linhart, L. J. Phillips, K. Durose, P. A. Stampe, R. J. Kennedy, D. O. Scanlon, G. Vardar, R. L. Field et al., Growth, disorder, and physical properties of ZnSnN₂, Appl. Phys. Lett. 103, 042109 (2013).
- [8] Veal, T. D., Feldberg, N., Quackenbush, N. F., Linhart, W. M., Scanlon, D. O., Piper, L. F., & Durbin, S. M. (2015). Advanced Energy Materials, 5.
- [9] W. Schockley; and H. J. Queisser, J. Appl. Phys., 1961, 32, 510–519.

- [10] T. Tiedje, E. Yablonovich, G. D. Cody and B. G. Brooks, IEEE Trans. Electron Devices, 1984, 31, 711–716.
- [11] S. P. Bremner, M. Y. Levy and C. B. Honsberg, Prog. Photovoltaics, 2008, 16, 225–233.
- [12] S. P. DenBaars, D. Feezell, K. Kelchner, S. Pimputkar, C.-C. Pan, C.-C. Yen, S. Tanaka, Y. Zhao, N. Pfaff, R. Farrell, M. Iza, S. Keller, U. Mishra, J. S. Speck and S. Nakamura, Acta Mater., 2013, 61, 945–951.
- [13] Quayle, P. C., Blanton, E. W., Punya, A., Junno, G. T., He, K., Han, L., Kash, K. (2015). Physical Review B,91(20), 205207.
- [14] Paul C. Quayle, Keliang He, Jie Shan and Kathleen Kash (2013). Synthesis, lattice structure, and band gap of ZnSnN₂. MRS Communications, 3, pp 135-138. doi:10.1557/mrc.2013.19.
- [15] Fioretti et al. (2015). Combinatorial insights into doping control and transport properties of zinc tin nitride. *Journal of Materials Chemistry C*,3(42), 11017-11028.
- [16] Kresse, G. & Joubert, D. From ultrasoft pseudopotentials to the projector augmentedwave method, Physical Review B 59, 1758–1775 (1999)
- [17] Kresse, G. & Furthmüller, J. Efficient iterative schemes forab initiototal-energy calculations using a plane-wave basis set, Physical Review B 54, 11169–11186 (1996)
- [18] J. Perdew, K. Burke, and M. Ernzerhof, Generalized Gradient Approximation Made Simple, Physical Review Letters 77, 3865 (1996)
- [19] Punya et. al Phys. Rev. B 84 (2011), Phys. Rev. B 84, 165204
- [20] P. Kraft, A. Bergamaschi, C. Broennimann, R. Dinapoli, E. F. Eikenberry, B. Henrich, I. Johnson, A. Mozzanica, C. M.Schleputz, P. R. Willmott, and B. Schmitt, J. Synchrotron Radiat. 16, 368 (2009).
- [21] C. M. Schlep"utz, R. Herger, P. R. Willmott, B. D. Patterson, O. Bunk, C. Br"onnimann, B. Henrich, G. H"ulsen, and E. F. Eikenberry, Acta Cryst. A 61, 418 (2005).
- [22] C. M. Schlep"utz, S. O. Mariager, S. A. Pauli, R. Feidenhans'l, and P. R. Willmott, J. Appl. Crystallogr. 44, 73 (2011).
- [23] Growth, disorder, and physical properties of ZnSnN₂, Feldberg, N. and Aldous, J. D. and Linhart, W. M. and Phillips, L. J. and Durose, K. and Stampe, P. A. and Kennedy, R. J. and Scanlon, D. O. and Vardar, G. and Field, R. L. and Jen, T. Y. and Goldman, R. S. and Veal, T. D. and Durbin, S. M., Applied Physics Letters, 103, 042109 (2013), DOI:http://dx.doi.org/10.1063/1.4816438
- [24] S. Francoeur, G. A. Seryogin, S. A. Nikishin, H. Temkin, Appl. Phys. Lett. 2000, 76, 2017.
- [25] See supplementary material at http://dx.doi.org/10.1063/1.4960109 for information on

the relationship between space group permutations of Pna2 $_1$ and Pmc2 $_1$ orthorhombic space groups, θ -2 θ measurements and pole figure plots showing two-fold symmetry in ZnSnN $_2$ films deposited on LiGaO $_2$ substrates.

Erratum:

https://doi.org/10.1063/1.5082196

- (1) Lattice constants in Table 11 are referenced in the Pbn21 structure and not Pna21 as earlier stated.
- (2) Per supplementary Figure 2; The film Bragg peaks expected in the Pn21a symmetry along the [00L] direction are of the form L=2n, where n is an integer and not L=4n as earlier stated. The (002) and (006) film Bragg peaks though present, have negligible structure factor in the Pn21a symmetry.

Both these corrections are typographical errors that do not affect the validity of results in the original article.

- 1 N. Senabulya, N. Feldberg, R. A. Makin, Y. Yang, G. Shi, C. M. Jones, E. Kioupakis, J. Mathis, R. Clarke, and S. M. Durbin,
- "Stabilization of orthorhombic phase in single-crystal ZnSnN2 films," AIP Adv. 6, 075019 (2016).
- 2158-3226/2018/8(12)/129901/1 **8**, 129901-1